



Fast inside-source X-ray fluorescent holography

 G. Bortel,^{a*} G. Faigel,^a M. Tegze^a and B. Angelov^b

^aInstitute for Solid State Physics and Optics, Wigner Research Centre for Physics, PO Box 49, H-1525 Budapest, Hungary, and ^bInstitute of Physics, ELI Beamlines, Academy of Sciences of the Czech Republic, Na Slovance 2, CZ-18221 Prague, Czech Republic. *Correspondence e-mail: bortel.gabor@wigner.mta.hu

Received 27 April 2018

Accepted 17 October 2018

Edited by Y. Amemiya, University of Tokyo, Japan

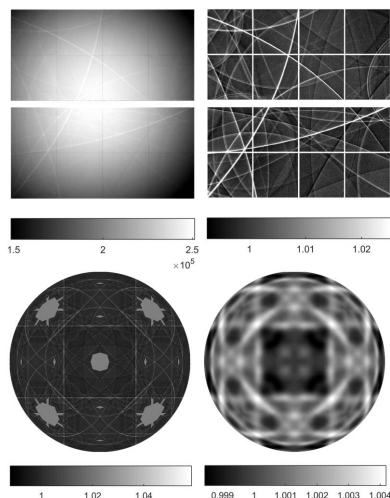
Keywords: X-ray holography; inside-source holography; X-ray free-electron laser.

Atomic resolution X-ray holography can be realized by using the atoms of the sample as inside sources or inside detectors. However, until now there were only very few experiments in which the atoms played the role of inside sources. The reason is twofold: (i) technically, inside-detector experiments are much easier and faster; (ii) by using atoms as inside detectors one can measure holograms at many energies on the same sample, which helps the reconstruction. This paper shows that, using new technical developments, inside-source holograms can be taken much faster than inside-detector holograms and, by applying a sophisticated evaluation method, high-quality reconstruction from a single-energy hologram can also be obtained.

1. Introduction

The knowledge of atomic and molecular structure is fundamental in physics, chemistry and biology. Therefore, in addition to traditional X-ray diffraction, several methods have been developed to recover the microscopic structure, one of them being atomic resolution X-ray holography. It is based on the holographic imaging principle, invented by Gabor 70 years ago (Gabor, 1948). The most important feature of the different variants of atomic resolution holography is the use of inside reference points (Szöke, 1986; Tegze & Faigel, 1996; Gog *et al.*, 1996). This means that selected atoms of the sample serve as point sources or point detectors of the hologram-forming waves.

Experimental demonstration of the inside reference point concept was carried out by Tegze & Faigel (1996) for inside sources and the collection of a single hologram took two months at a laboratory X-ray source. Using the same concept at a synchrotron source shortened the measuring time to six days (Hiort *et al.*, 2000). Experimental demonstration of the inside-detector concept was carried out by Gog *et al.* (1996), and the measurement time of a hologram was shortened to a few hours. In the following years many holographic experiments were performed; however, the inside-detector arrangement was almost exclusively used. There is one practical advantage of using atoms as inside detectors: one can take holograms of the same sample at various energies. Combining these holograms in the evaluation process facilitates artefact-free reconstruction, although this comes at a price; in these measurements the spatial-resolution elements (a pixel of the two-dimensional holographic image) must be measured using a serial approach while the sample is rotated about two axes (Faigel & Tegze, 1999). This results in relatively long measurement times considering the number of counts needed to have good enough statistics to see the small-amplitude holographic signal. The long measurement time and



the relatively complicated experimental setup hindered the application of holography. Most of the recent applications came from a Japanese group [for a review, see Hayashi & Korecki (2018)]. We expect much wider application by shortening the measuring time. This could be realized by applying the inside-source concept and measuring all the pixels in a parallel way. This type of experimental approach was used by Kopecky *et al.* (2001). They used an imaging plate for detection, and the collection time was about 1 h. Parallel detection would allow much shorter measuring times that are closer to ideal experimental conditions. One would expect a factor of 10^3 – 10^4 decrease in data collection time. This opens new possibilities for holographic studies. At a modern synchrotron source, a holographic pattern can be taken in less than a second. Furthermore, by using parallel detection one could introduce holographic measurements to X-ray free-electron lasers (XFELs), and collect a meaningful pattern with a single XFEL pulse. This creates many new applications, not possible by any other current methods. In this paper, we demonstrate experimentally that a hard X-ray holographic pattern can be taken in 1 s at a synchrotron source using the inside-source concept with a steady sample and parallel detection. We also introduce a new evaluation method, which allows us to obtain high-fidelity atomic images from single-energy holograms.

2. Experimental

Since we intend to demonstrate the feasibility of measuring a holographic pattern in a short time, we have chosen a sample which has already been measured. This allows us to compare the result with earlier measurements and validate our approach. Extended studies on NiO (Tegze *et al.*, 2000; Tegze & Faigel, 2001) have been made using the inside-detector method, and this sample has good characteristics for holographic studies so we used the same flat-plate single-crystal sample as in the earlier studies. The measurements were carried out at the ID18 beamline of ESRF. The experimental setup is shown in Fig. 1. The energy of the incident beam (14.4 keV) was defined by an Si(111) channel-cut monochromator. This beam was focused by a Kirkpatrick–Baez mirror to an approximately $5 \mu\text{m} \times 15 \mu\text{m}$ spot on the sample. The sample is fixed during the measurements; however, its relative orientation to the incident beam can be set by two axes, one vertical, which is parallel with the sample surface, and one perpendicular to it. Before the measurements, we set the orientation to avoid elastic diffraction peaks on the detector surface. We used an EIGER X 1M two-dimensional pixel detector from Dectris to collect the fluorescent photons. The detector-to-sample distance was 9 cm, the number of useful pixels is 1024×1024 of $75 \mu\text{m}$ size, and the average number of photons per pixel per second was 2×10^5 . This allowed us to collect a large enough solid angle to find symmetry elements in the measured pattern, which allows the extension of the hologram to the full solid angle (Faigel & Tegze, 1999; Tegze *et al.*, 1999). A single image with proper statistics to holography was taken in 1 s. In a recent experi-

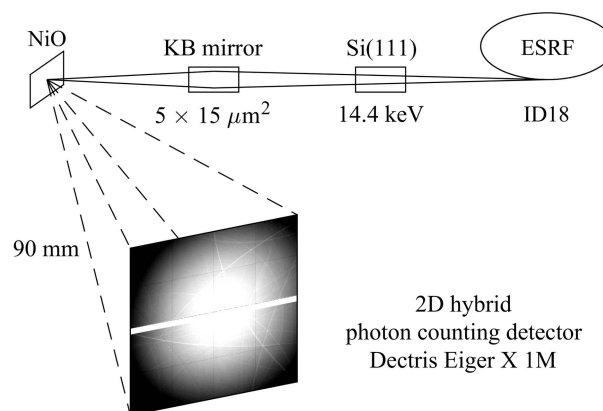


Figure 1

Experimental setup. A focused monochromatic synchrotron X-ray beam was used to excite Ni atoms in the sample. The emitted fluorescent radiation and its modulation due to interference were recorded with a two-dimensional pixel detector. The energy spectrum was monitored using a point detector.

ment (Ang *et al.*, 2018), a two-dimensional detector was used for collecting X-ray holographic data. However, this paper concentrates on the detection of valence sensitivity, using a different experimental setup not optimized for speed. This is reflected in the performance of the setup. A smaller area (256×256 pixels of $110 \mu\text{m}$ size) with much lower count rates ($50 \text{ photons pixel}^{-1} \text{ s}^{-1}$) than ours and a non-steady, scanned sample orientation was used, which led to a more than 1000 times longer measuring time. We also used this type of detector earlier in a similar experiment (Bortel *et al.*, 2016) and found that such a Medipix-based two-dimensional detector [this type was also used by Ang *et al.* (2018)] is not sufficient for holographic studies, being much more demanding than Kossel pattern collection.

3. Results

3.1. Hologram preparation

The raw intensity pattern was taken on a 1024×1024 -pixel grid. However, these data cannot be used directly for holographic back transform. Three preliminary steps must be carried out (Faigel & Tegze, 1999): (i) background correction, (ii) extension of the pattern to the full solid angle (Tegze *et al.*, 1999) and (iii) low-pass spatial filtering (Tegze *et al.*, 1999; Tegze, 2006). There are three effects that result in a spatially changing background: detector inhomogeneity, a geometrical factor caused by the varying solid angle seen by the pixels of the detector (due to both distance and incidence angle) and the absorption of the sample. In principle, one could use the flat-field correction provided with the detector for correcting the detector inhomogeneity. However, compared with the holographic signal, the factory-made correction is usually not good enough. Even if we could use the standard flat-field correction, in a second step we should correct for the geometrical factor. This can be achieved by fitting an analytical function on the smoothly varying part of the pattern. The form of this function can be determined from the geometry of

the experiment. However, in practice it is difficult to determine the perfect form of this function. Therefore, we used an experimental approach for background correction: we rotated the sample about the axis perpendicular to its surface. In this way the holographic oscillations are averaged, and only the geometry of the experiment and the pixel inhomogeneity remain. We used this pattern for normalization. Note that for correction one could also use a pattern from an amorphous sample with similar composition to the sample. However, in this case the amorphous sample has to be within the same geometrical conditions as that of the real sample. We have checked both approaches and found that the rotation method works better. In the resulting pattern, aside from the holographic signal, we may find weak Bragg peaks. The parts where these peaks are present (usually less than 5% of the total detector area) were left out as not measured points. This does not cause significant error in the final pattern, since in the next step of evaluation most of these left-out parts are filled in from symmetry equivalent points. Those points, which do not have any contribution from the measurement, are left out in the reconstruction process. To extend the hologram to the full solid angle, we use the symmetry elements of the pattern. To determine their exact location, a complete Kossel line pattern is fitted to the narrow intensity features present in the background-corrected image. Then the measured pattern is transformed to all symmetry equivalent orientations (resulting in multiple overlap in most regions) and then averaged to a common grid on the full sphere, on which the structure reconstruction is performed. This step is combined with the last step of preliminary data handling, application of a low-pass spatial filtering (convolution with a 5° FWHM Gaussian) to suppress the contribution of faraway atoms (Faigel & Tegze, 1999). The steps of the preliminary data handling are shown in Fig. 2.

3.2. Structure reconstruction

At this point, we arrived at a hologram (Fig. 2, bottom right panel) which can be used for reconstruction. There are several approaches for reconstruction: the simplest and most commonly used is the direct Helmholtz–Kirchhoff transformation (Faigel & Tegze, 1999; Born & Wolf, 1959). This is a deterministic method; it does not involve any iteration or optimization procedure. In this sense it is an unbiased approach, but one cannot include any additional knowledge about the sample that would facilitate the evaluation process. The twin-image problem is an inherent feature of holographic imaging (Faigel & Tegze, 1999) which leads to artefacts or distortion in the reconstructed image. If we want to avoid this disturbing effect, we have to include some additional knowledge about the sample in the evaluation process, or use more measurements, for example, holograms taken at different wavelengths (Barton, 1991; Faigel & Tegze, 1999). Holograms at various wavelengths can be easily obtained using the inside-detector arrangement (Gog *et al.*, 1996; Faigel & Tegze, 1999). However, in the case of inside-source holography, the energy of the hologram-forming waves is determined by the fluor-

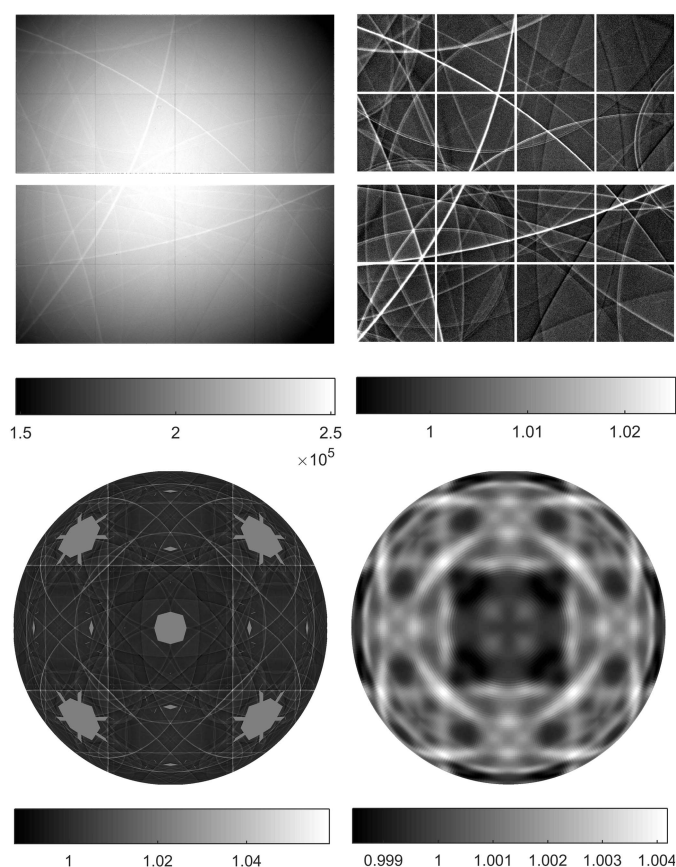


Figure 2
Steps of the data preparation. Top left: raw detector image. Top right: normalized image. Bottom left: hologram expanded to a sphere. Bottom right: low-pass filtered hologram.

escent energies of the source atoms. This may lead to the mixing of holograms with various energies in a single pattern if the detector cannot separate the fluorescent lines. Even if we could separate the fluorescent lines, we cannot freely choose several energies, only the few fluorescent lines given by the source atoms. Therefore, we have only one choice to avoid distortions in the reconstructed image: we have to use all available *a priori* information on the sample. In the first approximation, we evaluate the hologram as a single-energy hologram because the fluorescence is dominated by the close $K\alpha_{1,2}$ lines; furthermore we do not include any additional knowledge about the sample. We add the crystallinity and $K\beta$ contribution as an *a priori* knowledge in subsequent steps.

Considering all of this, we converted the holographic problem to a linear algebraic equation system, which was achieved by representing the charge density on a cubic grid, while the reciprocal-space grid was given by the points of measurement, more precisely the grid of the extended hologram. In mathematical form, the basic equation has the following form,

$$\chi_i = \sum_j H_{ij} \rho_j, \quad (1)$$

where $H_{ij} = 2P_{ij}(r_0/r_j) \text{Re} \exp[i(kr_j - \mathbf{k}_i \cdot \mathbf{r}_j)]$ is the holography matrix, $\rho_j = \rho(\mathbf{r}_j)$ is the charge density at point \mathbf{r}_j , $\chi_i = \chi(\mathbf{k}_i)$

is the measured holographic signal at point \mathbf{k}_i , $P_{ij} = (1/2)[1 + (\mathbf{k}_i \mathbf{r}_j / kr_j)^2]$ is the polarization factor, k is the absolute value of \mathbf{k}_i (constant, independent of i), $r_j = |\mathbf{r}_j|$ and r_0 is the classical electron radius (Faigel & Tegze, 1999). The sum is over all \mathbf{r}_j grid points. For given grids H_{ij} is constant, independent of the actual hologram. H_{ij} is usually not a well conditioned matrix (and in most cases it is underdetermined), therefore the solution of equation (1) (the unknown ρ) is not trivial. We used two approaches: the maximum entropy method (MEM) (correction free generalized iterative scaling; Curran & Clark, 2003) and the L1 minimization (iterative shrinkage thresholding method; Yang *et al.*, 2010). For X-ray holographic evaluation, maximum entropy has been used earlier by Matsushita *et al.* (2008) in combination with the scattering pattern extraction algorithm (SPEA), and recently L1-type iteration by the same group (Matsushita *et al.*, 2018). Our MEM and L1 implementation is different from their approach. We do not use SPEA and the inclusion of the crystallinity is radically different from the approximate translational symmetry introduced by Matsushita and co-workers. In contrast to Matsushita's work, we use exact translational symmetry by defining a new holography matrix. To see these differences more clearly, we briefly describe the implementation of our iteration method.

In the case of maximum entropy, the electron density must satisfy the conditions $\sum_j \rho_j = 1$ and $\rho_j \geq 0$. In practice, it means that we have to know the average electron density and the modeling volume. Knowing the composition of the sample, we have a very good first approximation for the electron density. The volume is given by the space in which we intend to find the atomic positions. In the case of L1 minimization, the condition for electron density is that $\sum_j |\rho_j|$ is minimal. This condition emphasizes the atomicity, *i.e.* it would put charges only to the smallest number of positions necessary to describe the measurement and zero otherwise. We found that in the very basic form both methods give lots of artefacts and the closest atoms (with small deviations from the exact positions) and other atoms are missing from the reconstructed image. Therefore, we included one more piece of information about the sample, the crystallinity. This means periodic electron density, not in the mathematical sense (not infinite periodicity), but at least in a short range about the central source atom in the modeling volume. This resulted in a change of the form of the holography matrix H_{ij} to $\tilde{H}_{ij} = 2P_{ij} \sum_l r_0 / r_{jl} \text{Re} \exp[i(kr_{jl} - \mathbf{k} \cdot \mathbf{r}_{jl})]$, where the sum over l is for the unit cells, and in this case formula (1) is transformed to

$$\chi_i = \sum_j \tilde{H}_{ij} \tilde{\rho}_j, \quad (2)$$

where $\tilde{\rho}_j$ is valid in a single unit cell and j runs over the gridpoints within this cell.

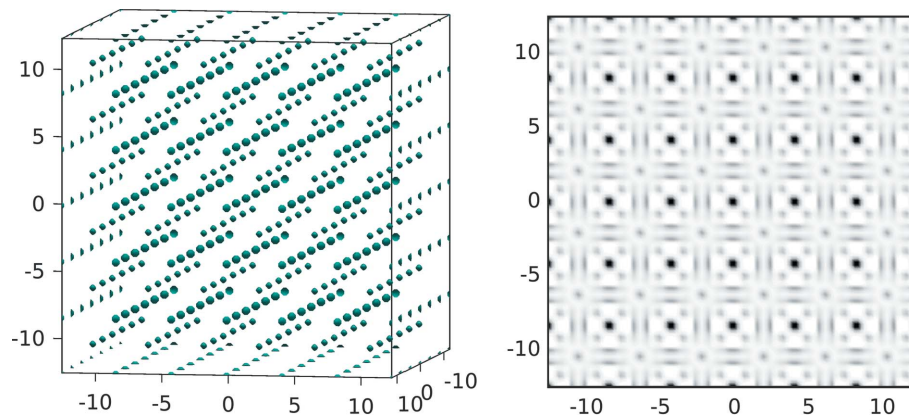


Figure 3
Reconstructed electron density. Left: isosurface plot of the reconstructed charge density. Right: charge density in a plane crossing the origin.

With this addition, both methods work and converge to similar electron densities. Therefore, here we show the result of the maximum entropy method only. The hologram of NiO and the reconstructed images are shown in the bottom right panel of Figs. 2 and 3, respectively.

Fig. 3. shows the reconstruction in the $6 \times 6 \times 6$ unit-cell volume as an isosurface at 30% of the maximum density (left panel). Aside from the three-dimensional picture, the (001) atomic plane at $z = 0$ height is also shown as a density map (right panel). It is easier to see on this cross section that the atoms at the face-centered positions are weaker. The reason for this is that these positions are close to the distance where the twin image cancels the real image (Faigel & Tegze, 1999). Using a single energy for reconstruction, this effect cannot be fully avoided. Otherwise, both the maximum entropy and L1 minimization give well located atomic positions. Unfortunately, the oxygen atoms cannot be identified because their scattering cross section is much smaller than that of nickel atoms. We checked whether a more refined evaluation could lead to the appearance of oxygen atoms. Therefore, the next step of our evaluation included the contribution from the $K\beta$ fluorescence, although this did not result in appreciable change in the reconstruction. This means that the measured pattern contains some error, which is comparable with the contribution coming from the $K\beta$ radiation. According to our analysis, this is not a statistical but a systematic error caused by detector imperfection and the limited solid angle accepted by the detector.

4. Conclusions

In this paper we have shown that high-fidelity atomic positions can be reconstructed from a single-energy hard X-ray hologram by using the inside-source concept. We also demonstrated that a statistically meaningful pattern can be taken in 1 s at ESRF. Taking into account that the number of photons in 1 s at ESRF is about the same as that in a single pulse of an XFEL source ($\sim 10^{12}$ photons), we expect that a hologram can be taken during a single pulse at XFELs. It is clear that our photon-counting detector will not work with a single pulse.

However, we expect that the recently developed integrating detectors, such as the Adaptive Gain Integrating Pixel Detector at EuXFEL (Becker *et al.*, 2012), can handle the high number of photons per pixel with low enough noise to see the holographic signal. This opens a series of new possibilities in structural studies. For example, one can obtain three-dimensional structural information of very short lived transient structures, appearing in highly non-ambient conditions: high pressure, high magnetic fields, high temperatures, where experimental conditions cannot be repeated with exact control.

Funding information

The financial support of NKFIH K115504 grant: VEKOP-2.3.3-15-2016-00001, the beam time given by ESRF and the help of A. Chumakov at the ID18 beamline are acknowledged. BA is supported by the Czech Science Foundation Grant (grant No. GACR 17-00973S) and the European Commission funded projects ELI, Extreme Light Infrastructure, phase 2 (CZ.02.1.01/0.0/0.0/15_008/0000162) and ELIBIO (CZ.02.1.01/0.0/0.0/15_003/0000447) from the European Regional Development Fund.

References

Ang, A. K. R., Matsushita, T., Hashimoto, Y., Happo, N., Yamamoto, Y., Mizuguchi, M., Sato-Tomita, A., Shibayama, N., Sasaki, Y. C., Kimura, K., Taguchi, M., Daimon, H. & Hayashi, K. (2018). *Phys. Status Solidi B*, doi:10.1002/pssb.201800100.

Barton, J. J. (1991). *Phys. Rev. Lett.* **67**, 3106–3109.

Becker, J., Greiffenberg, D., Trunk, U., Shi, X., Dinapoli, R., Mozzanica, A., Henrich, B., Schmitt, B. & Graafsma, H. (2012). *Nucl. Instrum. Methods Phys. Res. A*, **694**, 82–90.

Born, M. & Wolf, E. (1959). *Principles of Optics*. London: Pergamon.

Bortel, G., Faigel, G., Tegze, M. & Chumakov, A. (2016). *J. Synchrotron Rad.* **23**, 214–218.

Curran, J. R. & Clark, S. (2003). *Proceedings of the Tenth Conference on European Chapter of the Association for Computational Linguistics (EACL'03)*, Vol. 1, pp. 91–98. Association for Computational Linguistics, Stroudsburg, PA, USA.

Faigel, G. & Tegze, M. (1999). *Rep. Prog. Phys.* **62**, 355–393.

Gabor, D. (1948). *Nature*, **161**, 777–778.

Gog, T., Len, P. M., Materlik, G., Bahr, D., Fadley, C. S. & Sanchez-Hanke, C. (1996). *Phys. Rev. Lett.* **76**, 3132–3135.

Hayashi, K. & Korecki, P. (2018). *J. Phys. Soc. Jpn.* **87**, 061003-1–11.

Hiort, T., Novikov, D. V., Kossel, E. & Materlik, G. (2000). *Phys. Rev. B*, **61**, R830–R833.

Kopecky, M., Busetto, E., Lausi, A., Miculin, M. & Savoia, A. (2001). *Appl. Phys. Lett.* **78**, 2985–2987.

Matsushita, T., Guo, F. Z., Suzuki, M., Matsui, F., Daimon, H. & Hayashi, K. (2008). *Phys. Rev. B*, **78**, 144111-1–8.

Matsushita, T., Muro, T., Matsui, F., Happo, N., Hosokawa, S., Ohoyama, K., Sato-Tomita, A., Sasaki, Y. C. & Hayashi, K. (2018). *J. Phys. Soc. Jpn.* **87**, 061002-1–11.

Szöke, A. (1986). *AIP Conf. Proc.* **147**, 361–367.

Tegze, M. (2006). *Phys. Rev. B*, **73**, 214104-1–6.

Tegze, M. & Faigel, G. (1996). *Nature*, **380**, 49–51.

Tegze, M. & Faigel, G. (2001). *J. Phys. Condens. Matter*, **13**, 10613–10623.

Tegze, M., Faigel, G., Marchesini, S., Belakhovsky, M. & Chumakov, A. I. (1999). *Phys. Rev. Lett.* **82**, 4847–4850.

Tegze, M., Faigel, G., Marchesini, S., Belakhovsky, M. & Ulrich, O. (2000). *Nature*, **407**, 38.

Yang, A., Ganesh, A., Sastry, S. & Ma, Y. (2010). Technical Report No. UCB/EECS-2010-13. Electrical Engineering and Computer Sciences University of California at Berkeley, USA.